

Two of a Kind—The Biosynthetic Pathways of Chlorotonil and Anthracimycin

Katrin Jungmann,[†] Rolf Jansen,[‡] Klaus Gerth,[‡] Volker Huch,[†] Daniel Krug,[†] William Fenical,[§] and Rolf Müller^{*,†}

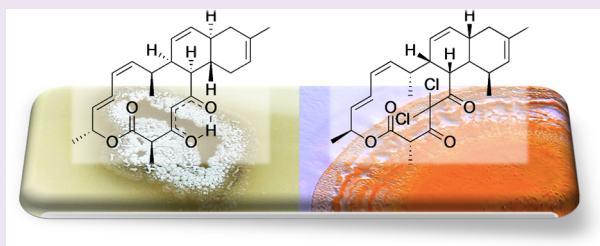
[†]Department of Microbial Natural Products, Helmholtz Institute for Pharmaceutical Research Saarland, Helmholtz Centre for Infection Research and Pharmaceutical Biotechnology, Saarland University, Saarbrücken, Germany

[‡]Helmholtz Centre for Infection Research, Department of Microbial Drugs, Braunschweig, Germany

[§]Center for Marine Biotechnology and Biomedicine, Scripps Institution of Oceanography, University of California, San Diego, La Jolla, California, United States

S Supporting Information

ABSTRACT: Chlorotonil A is a novel polyketide isolated from the myxobacterium *Sorangium cellulosum* So ce1525 that features a unique gem-dichloro-1,3-dione moiety. It exhibits potent bioactivity, most notably against the problematic malaria pathogen *Plasmodium falciparum* in the nanomolar range. In addition, strong antibacterial and moderate antifungal activity were determined. The outstanding biological activity of chlorotonil A as well as its unusual chemical structure triggered our interest in elucidating its biosynthesis, a prerequisite for alteration of the scaffold by synthetic biology approaches. This endeavor was facilitated by a recent report describing the strikingly similar structure of anthracimycin from a marine streptomycete, a compound of considerable interest due to its potent antibacterial activity. In this study, we report the identification and characterization of the chlorotonil A biosynthetic gene cluster from So ce1525 and compare it with that for anthracimycin biosynthesis. Access to both gene clusters allowed us to highlight commonalities between the two pathways and revealed striking differences, some of which can plausibly explain the structural differences observed between these intriguing natural products.



In light of the alarming resistance rates for clinical antibiotics, and the concomitant loss of formerly potent therapy options, there is an increasing demand to identify new anti-infective drugs. Natural products such as secondary metabolites isolated from bacteria have proven to be a fruitful source of new lead structures for drug discovery. Evolutionarily preselected for potent biological activity, natural products are considered as “privileged structures” in the fight against resistant pathogens as they provide an increased chance to hit previously unknown targets.¹ Over the past two decades, myxobacteria have been established as a rich source of novel bioactive compounds, suggesting great potential for the discovery of new drug candidates with unusual modes of action.² In particular, strains of the genus *Sorangium* have been frequently reported as promising producers of novel secondary metabolites with potent biological activity.³ The remarkably large genome size of members of *Sorangium* species is thought to reflect their capacity for secondary metabolite biosynthesis.⁴ A broad screening program for bioactive secondary metabolites from *Sorangium* strains led to the isolation of chlorotonil A from *Sorangium cellulosum* So ce1525 in 2008.⁵ Structure elucidation identified the highly lipophilic macrolide chlorotonil A which features a unique gem-dichloro-1,3-dione structural moiety. This structural feature is novel among natural polyketides and fueled our interest in elucidating the chlorotonil biosynthetic pathway. Strong

antibacterial activity as well as a high potency against the malaria pathogen *Plasmodium falciparum* shown in mouse models fortified our interest, as did the report of the strikingly similar marine metabolite anthracimycin in 2013.⁶ Anthracimycin shows good antibacterial activity which could be enhanced via chemical dichlorination of the scaffold, resulting in a derivative structurally mimicking chlorotonil A.

Polyketide metabolites such as chlorotonil A and anthracimycin are produced by modular polyketide synthases (PKS), which catalyze the stepwise connection of simple precursor molecules followed by distinct enzymatic tailoring reactions to form complex natural products. Each extension cycle is catalyzed by a set of enzymatic domains which are grouped into modules to form a biosynthetic assembly line. In the last module, the product is most commonly released from the assembly line as either a linear or circular product. Modification of the polyketide core structure by free-standing enzyme functionalities can occur during or after assembly on the PKS. A special subtype of polyketide biosynthesis gene clusters, namely the *trans*-AT type clusters, have been discovered and investigated in

Received: July 8, 2015

Accepted: August 29, 2015

Published: September 8, 2015



the past couple of years.⁷ In these PKSs, the individual modules lack integral acyltransferase (AT) domains for selection of the carboxylic acid substrate required for chain elongation; instead, a discrete AT encoding gene encoded in close proximity to the PKS genes, the product of which is responsible for iterative extender unit selection and transfer, can be found. To date, only a small number of *trans*-AT PKS systems have been explored in detail, and their mechanism of product assembly is currently not fully understood.

Understanding and elucidating the biosynthesis of chlorotoniol A and anthracimycin sets the stage for the bioengineering of novel derivatives using synthetic biology approaches. Here, we report the identification of the chlorotoniol A biosynthetic pathway in *Sorangium cellulosum* So ce1525 and provide the first insights into its biosynthesis. Gene inactivation experiments and feeding studies were performed to corroborate our findings. A detailed comparison with the biosynthetic pathway of anthracimycin found in *Streptomyces* CNH365 sheds light on production of these intriguingly similar compounds by different hosts from different habitats.

RESULTS AND DISCUSSION

Identification of the Chlorotoniol Biosynthetic Gene Cluster and New Chlorotoniol Congeners. We sought to identify the gene cluster responsible for chlorotoniol biosynthesis in the genome of *Sorangium cellulosum* So ce1525 and initially conducted 454 pyrosequencing for this purpose. The resulting 138 scaffolds were screened for putative PKS pathways matching the retro-biosynthetic proposal for chlorotoniol synthesis. As the dichloro-pattern in chlorotoniol A suggests involvement of a halogenating enzyme, all scaffolds were additionally searched for genes putatively encoding a halogenase. Using this approach, a concordant gene cluster harboring a putative halogenase gene as well as a tandem-AT domain encoding gene were found colocalized on one scaffold. In order to probe the involvement of this locus in chlorotoniol biosynthesis through gene inactivation, multiple conditions for directed mutagenesis of So ce 1525 were evaluated. After establishing a suitable method for conjugational DNA transfer, targeted disruption of the putative tandem AT domain encoding gene was performed by insertion of a hygromycin cassette using single-crossover homologous recombination (Figure 1). The resulting So ce1525 mutant phenotype showed no production of chlorotoniol A and thus confirmed the identification of the chlorotoniol biosynthesis gene cluster. However, insufficient sequence quality precluded in-depth *in silico* analysis of the genomic locus. Gap-closing was therefore performed using PCR and by additional sequencing from a cosmid library (Figure S10). Moreover, comparative LC-MS analysis of extracts from wildtype and mutant cultures highlighted several signals showing *m/z* values and isotope patterns suggestive of chlorotoniol congeners not previously reported (Table 1 and the Supporting Information). Isolation and structural elucidation was pursued for three chlorotoniol candidates which became accessible from a large-scale fermentation of the wildtype strain, revealing the structures of new chlorotoniols B, C, and C2 (Supporting Information).

Besides its outstanding antimalarial activity,⁸ chlorotoniol A also exhibits remarkable antibacterial activity. Since solubility of the compound in polar solvents is very poor, a formulation in THF and cremophor was developed and used for antimicrobial *in vitro* assays (minimum inhibitory concentration, MIC). Overall, the compound strongly inhibited Gram-positive indicator strains such as *Bacillus subtilis* and *Staphylococcus aureus* in the

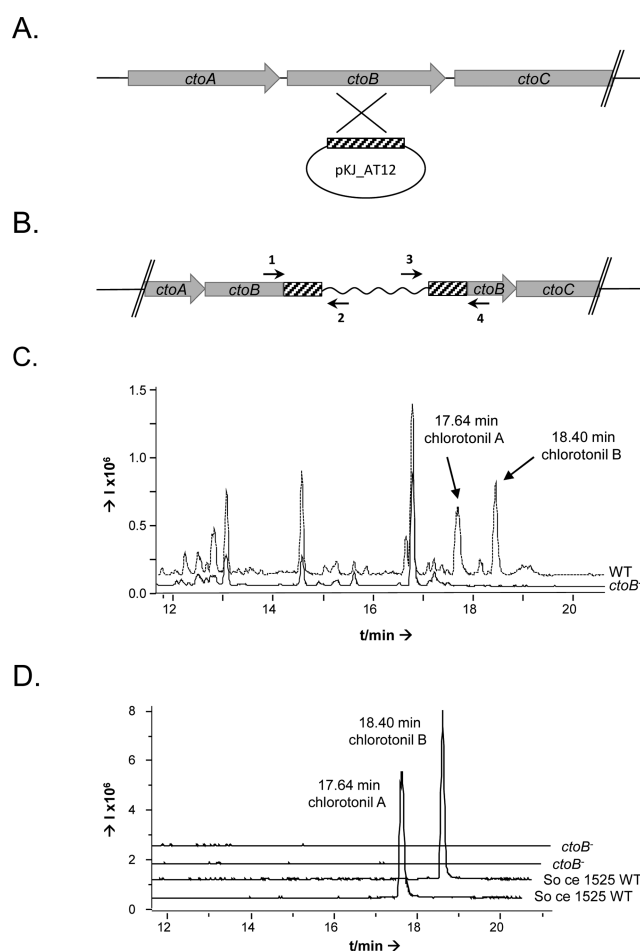
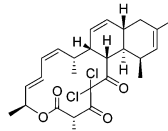
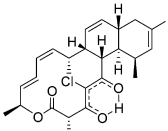
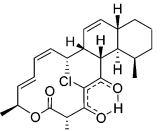
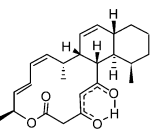


Figure 1. Strategy for the targeted inactivation of *ctoB* in the chlorotoniol A biosynthetic gene cluster. (A) Schematic overview on the gene organization at the 5' end of the gene cluster and the construct *pKJ_AT12* designed for *ctoB* inactivation via single crossover insertion. (B) Genetic organization of the mutant strain *So ce1525 CtoAT::pKJ_AT12* containing the integrated *pKJ_AT12*. For verification of the genotype, PCR analysis was used (Figure S1). The primers used are indicated by the arrows (1, *AT_KO_ver_fwd*; 2, *pSUP_Hyg_rev*; 3, *pSUPHyg_fwd*; 4, *AT_KO_ver_rev*). (C) Analysis of chlorotoniol production of *So ce1525* wildtype in comparison to the tandem AT knockout mutant by HPLC. Base peak chromatograms (200–500 Da) of the wildtype strain *So ce1525* showing production of chlorotoniol A and B (upper dashed line) and the mutant strain lacking production of chlorotoniols. (D) Extracted ion chromatograms of the chlorotoniol A target mass 479.175 *m/z* [*M* + *H*]⁺ and the chlorotoniol B target mass 445.214 *m/z* [*M* + *H*]⁺ are shown for the wildtype (lower lines) and the mutant strain.

low nanogram per milliliter range and displayed moderate antifungal activity, while cytotoxicity against established cell lines was found to be relatively low (IC₅₀ for CHO-K1 and HCT-116 cells >5 μ M). It is notable that the MIC values of the dichlorinated chlorotoniol A are significantly higher than those determined for the mono- and nonchlorinated congeners. This indicates that the chlorine atoms are crucial for the bioactivity, which is also supported by the results from antimalaria testing.⁸ Other than for anthracimycin, no activity against Gram-negative bacteria could be found.

In Silico Analysis of the *cto* Biosynthetic Gene Cluster and Model for Chlorotoniol Biosynthesis. The chlorotoniol biosynthetic gene cluster as identified by sequencing and confirmed through gene inactivation spans 80.7 kbp and contains 21 genes, among which three large genes (*ctoC*, *ctoD*, *ctoE*; Table 2)

Table 1. Bioactivity Testing of Chlorotonil A and Its Congeners

Table 1. Bioactivity testing of chlorotonil A and its congeners								
	Chlorotonil A 1		Chlorotonil B 2		Chlorotonil C 3		Chlorotonil C2 4	
								
MIC	$\mu\text{g/ml}$	μM	$\mu\text{g/ml}$	μM	$\mu\text{g/ml}$	μM	$\mu\text{g/ml}$	μM
<i>M. luteus</i> DSM-1790	0.0125	0.025	> 3.2	>6.4	> 3.2	>6.4	1.6	3.8
<i>B. subtilis</i> DSM-10	≤ 0.003	≤ 0.006	> 3.2	>6.4	> 3.2	>6.4	1.6	3.8
<i>S. aureus</i> Newman	0.006	0.012	> 3.2	>6.4	3.2	>6.4	1.6	3.8
<i>E. faecalis</i> ATCC-29212	> 3.2	>6.4	> 3.2	>6.4	> 3.2	>6.4	> 3.2	>6.4
<i>S. pneumoniae</i> DSM-20566	0.0125	0.025	> 3.2	>6.4	> 3.2	>6.4	> 3.2	>6.4
<i>E. coli</i> (TolC-deficient)	> 3.2	>6.4	> 3.2	>6.4	> 3.2	>6.4	> 3.2	>6.4
<i>E. coli</i> DSM-1116	> 3.2	>6.4	> 3.2	>6.4	> 3.2	>6.4	> 3.2	>6.4

encode a 10-modular PKS. As none of the PKS modules contain an integral AT domain, the megaenzyme complex is assigned to the group of *trans*-AT PKSs. In *trans*-AT pathways, the AT functionality is absent from individual modules and is replaced by a tandem-AT domain, encoded by *ctoB* in the case of chlorotonil biosynthesis. Alignment of the two AT domains with other known AT domains from *trans*-AT PKS gene clusters reveals that the AT2 domain falls into the malonyltransferase clade and is consequently responsible for extender unit selection (Figure S2). This finding is underpinned by the presence of the common GHSxG motif in AT2, which is altered to GASxG in AT1. The AT1 domain groups with domains of the “acyl hydrolase” clade; AT domains belonging to this group exhibit a proof reading functionality by removing stalled acyl units from blocked carrier proteins.^{9,10} Thus, the didomain enzyme CtoB is most likely responsible for loading of the ACP domains with malonyl-CoA extender units and additionally exhibits a proof-reading functionality responsible for off-loading of deadlocked intermediates. As inferred from the chlorotonil structure, acetyl-CoA serves as a starter unit for the first module. Fused to the C-terminus of the tandem AT domain, an additional ER domain of the 2-nitropropane dioxygenase family can be found. A similar domain arrangement has also already been described for the mupirocin, pederin, chivosazol, and kirromycin pathways.^{11–14} For bacillaene, it could be shown that the ER domain fused to the *trans*-AT domain PksE was able to reduce double bonds in polyketide precursors independent from the action of the AT domain and thus acts as an additional *trans*-ER.¹⁵ In the case of chlorotonil biosynthesis, no such functionality is missing on the assembly line; hence the role of the *trans*-ER domain cannot be conclusively defined.

The presence of 10 active KS domains in the chlorotonil PKS, all exhibiting the highly conserved HGTGT motif, as well as the DxxCSSLx motif with slight variations (Figure S3) is in accordance with the retrobiosynthetic analysis that proposes the incorporation of 10 acetate-derived extender units.¹⁶ Substrate specificity of all 10 KS domains located on *ctoCDE* was predicted via multiple alignment according to Piel et al.,¹⁷ whereupon the prognosis largely matches the biosynthesis model for chlorotonil. (Figure S16). In the course of chlorotonil biosynthesis, the extender units are evidently processed by a reductive loop in eight out of 10 cases, which leads to either

α,β -olefinic or alkylc intermediates. Analysis of the KR domains present in CtoC,D,E revealed an LxD motif in all eight KR domains (KR in modules 2, 3, 4, 6, 7, 8); hence all of them belong to the class of B-type ketoreductases leading to S-configured alcohols.^{18,19} For KR1 and KR5, no such LxD motif could be detected, which assigns them to the group of A-type ketoreductases forming the respective R-configured alcohols.

Furthermore, eight modules of the chlorotonil PKS include DH domains, two of which are found on so-called split modules where the respective module stretches across two genes. Seven out of eight DH domains show the typical motifs needed for dehydratase activity, including highly conserved histidine and aspartate residues (Figure S3).²⁰ The deviating dehydratase domain in module one is a truncated variant of a DH domain lacking the essential motifs and conserved residues and is proposed to be inactive, in agreement with the chlorotonil structure. The only ER domain found in module six shows the conserved tyrosine residue correlated with 2S configuration in the polyketide, while only slight deviations in the LxHxxxGGVGxxxAXxxA NADPH binding site consensus motif can be observed (Figure S5); nevertheless its activity seems to be maintained during biosynthesis, as concluded from the reduction of the double bond introduced by module six. Intriguingly, this ER domain occupies an unusual position in relation to the surrounding domains: contrary to the canonical placement of ER domains in the reductive loop, this domain lies downstream of the ACP domain in module six. Compared to *cis*-AT PKS systems, this positioning seems rather unusual, but for *trans*-AT systems this domain arrangement has already been described, e.g., in the rhizopodin biosynthetic gene cluster.²¹ Whether this positioning influences domain activity or makes the ER available for processing reactions outside its ancestral module remains unclear. Our retrobiosynthetic analysis suggests that two double bond shifts are to be carried out in modules three and seven, to yield the respective α -methylated, β,γ -olefinic intermediate. Deviant from known mechanisms and domain architectures of the earlier described shift modules catalyzing this reaction, as for example known from rhizoxin biosynthesis, no such enzymatic activity can be found in the two modules.²² It is thus very likely that the double bond shift is executed in the respective elongating module as previously described for bacillaene biosynthesis.²³ Split modules in which one module is partitioned between two

Table 2. Proposed Function of the Genes Involved in Chlorotoniol A Biosynthesis and the Surrounding Open Reading Frames

gene/protein	length (bp/aa)	proposed function			
<i>ctoA</i> /CtoA	1875/625	FAD-dependent halogenase			
<i>ctoB</i> /CtoB	3462/1154	AT ₁ (61–993), AT ₂ (1063–1884), ER (1920–3156)			
<i>ctoC</i> /CtoC	18816/6272	KS ₁ (19–1294), DH ₁ * (2650–3007), KR ₁ (3580–4135), ACP ₁ (4405–4609), KS ₂ (4774–6082), DH ₂ (6655–7483), KR ₂ (8320–8875), ACP ₂ (9211–9397), KS ₃ (9625–10930), ACP ₃₋₁ (11142–11325), DH ₃ (11838–12663), KR ₃ (13383–13920), MT ₃ (14622–15282), ACP ₃₋₂ (15504–15711), KS ₄ (16018–17281), DH ₄ (17893–18663)			
<i>ctoD</i> /CtoD	22806/7602	KR ₄ (862–1414), ACP ₄ (1699–1900), KS ₅ (2158–3457), DH ₅ (4015–4839), KR ₅ (5584–6139), ACP ₅ (6397–6595), KS ₆ (6766–8068), ACP ₆₋₁ (8242–8446), DH ₆ (8939–9762), KR ₆ (10525–11065), MT ₆ (11755–12343), ACP ₆₋₂ (12580–12790), ER ₆ (13096–14023), KS ₇ (14104–15379), DH ₇ (15928–16752), KR ₇ (17428–18022), MT ₇ (18721–19384), ACP ₇ (19516–19723), KS ₈ (19987–21256), DH ₈ (21829–22653)			
<i>ctoE</i> /CtoEC	7773/2591	KR ₈ (844–1393), ACP ₈ (1639–1837), KS ₉ (2008–3304), ACP ₉₋₁ (3496–3700), ACP ₉₋₂ (4324–4531), KS ₁₀ (4714–6019), ACP ₁₀ (6637–6838), TE (6943–7723)			
		proposed function of homologous protein	source of the homologous protein	identity/similarity, %	accession number (GenBank)
CtoF	828/276	SAM-dep. methyltransferase	<i>Thermicola potens</i>	41/59	WP_013119426
Orf1	765/255	hypothetical protein	<i>Mariiprofundus ferrooxydans</i>	48/70	WP_009850450
Orf2	1218/409	ABC transporter—permease	<i>Enhygromyxa salina</i>	26/44	KIG16386
Orf3	1233/411	ABC transporter—permease	<i>Enhygromyxa salina</i>	31/49	KIG16385
Orf4	696/232	ABC transporter—ATP binding protein	<i>Myxococcus xanthus</i>	49/61	WP_011552505
Orf5	1236/412	hypothetical protein	<i>Syntrophobacter fumaroxidans</i>	35/48	WP_011699354
Orf6	798/266	ATP binding protein	<i>Amicyclatopsis nigriscens</i>	60/74	WP_020673914
Orf7	702/234	putative ABC transporter	<i>Halococcus hamelinensis</i>	38/51	WP_007692158
Orf8	708/236	putative ABC transporter	<i>Methanocella arvoryzae</i>	28/46	WP_012036131
Orf9	591/197	esterase	<i>Sorangium cellulosum</i>	76/84	WP_012236733
Orf10	828/276	LuxR family transcriptional regulator	<i>Sorangium cellulosum</i>	83/87	WP_012236732
Orf11	657/219	hypothetical protein	<i>Chondromyces apiculatus</i>	73/82	EYF05039
Orf12	1680/560	hypothetical protein	<i>Chondromyces apiculatus</i>	74/82	EYF05038
Orf13	783/261	hypothetical protein	<i>Chondromyces apiculatus</i>	67/74	EYF05037

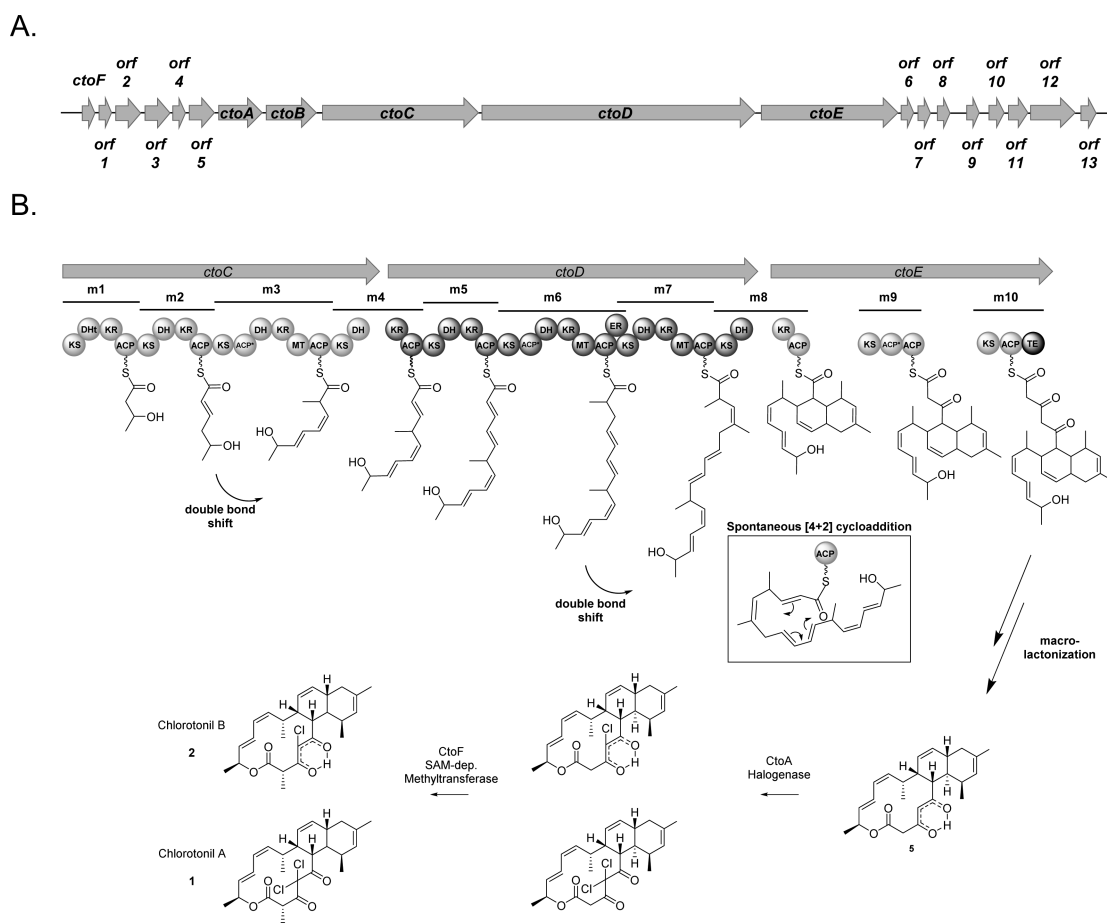


Figure 2. A model for chlorotonil biosynthesis in *So ce 1525*. The organization of the chlorotonil A biosynthetic gene cluster is shown in A. The proposed biosynthetic pathway for chlorotonil A and B is shown in B. ACP, acyl carrier protein; DH, dehydratase, DHT, inactive truncated dehydratase; ER, enoyl reductase; KR, keto reductase; KS, keto synthase; MT, methyl transferase; TE, thioesterase.

proteins are commonly observed in *trans*-AT PKS systems.⁷ Two split modules (module 4, module 8) are found in the chlorotonil PKS; this structural peculiarity does not seem to influence the construction of the polyketide chain as both modules yield the respective acrylyl intermediates corresponding to the degree of β -processing expected from the allocated KR and DH domains and stipulated by retro-biosynthetic analysis.

The domain architecture of the chlorotonil PKS diverges notably from the colinearity rule with three apparently superfluous ACP domains. Additional ACP domains have been proposed to play a role in β -branching events where they are described as a breakpoint for β -branch incorporation, facilitating this modification via retardation of biosynthetic flux through the pathway.²⁴ Furthermore, it has been speculated that these additional domains could enhance the yield in complex enzymatic reactions as described for curacin biosynthesis.²⁵ It is tempting to interpret the duplication of ACP domains in modules three and six accordingly, as the two modules harbor MT domains and are responsible for incorporation of an α -methyl branch. However, in contrast to all 10 other ACPs, the three duplicate ACP domains do not possess the conserved serine in the GIDSxL motif where the phosphopantetheinyl arm is attached.²⁶ Thus, they appear to be nonfunctional and may represent an inactive flanking subdomain of the upstream KS as previously reported by Keatinge-Clay et al.²⁷

Maturation of the PKS-derived Chlorotonil Core. The α -methyl branches at C8, C10, and C16 in chlorotonil A are

plausibly incorporated by the integral methyltransferase domains in modules three, six, and seven. Methylation at C2 is proposed as a post-PKS tailoring reaction catalyzed by the free-standing S-adenosylmethionine (SAM)-dependent methyltransferase CtoF. The SAM origin of all methyl groups was proven by a ¹³C-methyl-methionine feeding study (Figure S9). An alignment of all four MTs revealed that the three internal MT domains of modules three, six, and seven are highly similar to each other and distinct from the free-standing MT domain encoded by *ctoF* (Figures S6–S7.1). We reason that the three integral MT domains are responsible for α -methylation during polyketide chain formation at the appropriate positions, while the external methyltransferase CtoF acts upon the circular premature polyketide (1 in Figure 2). This assumption is supported by the finding of a mass of $[M + H]^+ = 397.23$ *m/z* representing a chlorotonil precursor molecule which is not halogenated at C4 and not methylated at C2, during LC-MS analysis of *So ce1525* extracts (Figure S13).

A striking feature of chlorotonil is its decalin ring partial structure, which likely results from an intramolecular Diels–Alder-like [4 + 2] cycloaddition reaction. We propose that this reaction takes place during polyketide assembly on the PKS enzyme complex. Whether such [4 + 2]-cycloadditions can occur spontaneously or involve enzymatic catalysis by so-called “Diels–Alderase” remains controversial. For lovastatin biosynthesis in *Aspergillus terreus*, a free-standing enoylreductase LovC is thought to assist the ring formation as a partner protein of

the lovastatin nonaketide synthase LovB,²⁸ whereas the methyltransferase homologue SpinF from *Saccharopolyspora spinosa* catalyzes an intramolecular Diels–Alder reaction leading to a spinosyn precursor molecule.²⁹ In addition, two distinct enzymes, namely the macrophomate synthase MPS (from *Macrophoma commelinae*)³⁰ and the solanopyrone synthase SolS (from *Alternaria solani*),³¹ have been recombinantly produced and associated with Diels–Alder-like biotransformations. Very recently, new enzymes involved in the macrocyclization of spirotetronate containing polyketides have been shown to catalyze [4 + 2] cycloadditions: in the case of versipelostatin, VstJ was found to catalyze ring formation between a highly flexible acyclic diene substructure and an exocyclic olefin.³² The distance and spatial arrangement between those two moieties seems to be the critical parameter, which necessitates enzymatic catalysis to accomplish ring formation. In-depth *in silico* analysis of the chlorotonil biosynthetic gene cluster and the genomic regions up- and downstream of this locus did not reveal any genes exhibiting significant homology to the aforementioned enzymes. We thus conclude that the intramolecular Diels–Alder reaction, leading to formation of the decalin moiety, occurs spontaneously without dedicated enzymatic catalysis while the polyketide chain is still tethered to the assembly line in module eight. In light of the heterogeneity of putative Diels–Alderase enzymes and their substrates reported to date, it seems likely that there is no generalized enzyme class to promote [4 + 2] cycloadditions. Especially in the case of versipelostatin it seems that the enzyme identified is highly specific for the versipelostatin precursor. As mentioned by the authors, it is very likely that VstJ orientates its substrate into an advantageous conformation for ring formation. In the case of chlorotonil, we hypothesize that the diene and the dienophile moiety could arrange in close proximity to each other while the polyketide intermediate is tethered to the ACP domain (Figure 2, Figure S11); thus additional enzymatic catalysis of the Diels–Alder reaction may not be necessary.

After 10 rounds of chain extension, the polyketide chain is released from the assembly line and cyclized by the TE domain of module 10. This premature macrolactone (**5** in Figure 2) then undergoes two tailoring steps to form chlorotonil A, and we propose the following timing for these post-PKS modifications: first, **5** is halogenated at the C3 position by the flavin dependent halogenase CtoA; second, the methylation at C2 occurs catalyzed by the free-standing methyltransferase CtoF to yield chlorotonil A. Evidence for this order of modification reactions comes from the structures of natural chlorotonil congeners as well as from feeding experiments and is discussed below. The highly abundant chlorotonil B and less abundant chlorotonil C differ from chlorotonil A by the lack of a second chlorine atom at C4. Chlorotonil C and C2 also exhibit carbon skeleton variations: the C10 methyl group and C9–C10 double bond are missing. For the biosynthesis of these derivatives, two possible scenarios are conceivable. First, the missing methyl group at C10, which results from inefficient methylation functionality in module seven, could transform the resulting polyketide into a substrate for an external hydrogenase that reduces the C9–C10 double bond. Second, we cannot exclude that the oddly positioned ER domain between modules six and seven accessorially acts upon the polyketide chain tethered in module seven when the α -methyl group is absent.

Geminal Dichlorination of the Chlorotonil Scaffold by the Halogenase CtoA. To the best of our knowledge, the unique gem-dichloro-1,3-dione substructure found in chlorotonil

A has not been reported for any other natural product. This feature appears critical to the bioactivity of chlorotonil as the antimalarial activity was lost when the nonhalogenated derivatives were examined.⁸ Similarly, the effectiveness of anthracimycin increased when the compound was chemically dichlorinated.⁶ To investigate the role of CtoA, a putative FAD-dependent halogenase, for chlorotonil halogenation we inactivated the *ctoA* gene via the established single crossover protocol: we expected that mutant strain would produce only nonhalogenated chlorotonil derivatives. Disappointingly, the resulting mutant produced no chlorotonil or analogues indicating a polar effect on the downstream genes. Despite numerous attempts a double-crossover excision of the halogenase gene did not succeed.

We then attempted reconstitution of the halogenation reaction *in vitro*, but efforts toward recombinant production of CtoA in *E. coli* were not successful. To corroborate our hypothesis for the timing of tailoring reactions during chlorotonil maturation, we instead used the tandem-AT (*ctoB*) knockout mutant in a feeding study to probe halogenation of chlorotonils B (**2** in Table 1) and C2 (**4** in Table 1). In the *ctoB* mutant, translation of *ctoA* is not hampered by a polar effect as it resides upstream of the disruption (Figure 2). After incubating the *ctoB* mutant with **2** and **4** for 10 days, extracts were analyzed for the presence of chlorinated compounds using LC-MS, but neither extract showed the presence of chlorotonil A. However, further analysis of the MS data from feeding **4** identified two conspicuous peaks with chlorotonil-like retention times and MS patterns consistent with the presence of halogen atoms. The *m/z* ratios of these, 433.21 and 467.17, respectively, were 14 mass units higher than the anticipated $[M + H]^+$ ions for mono- and dichlorination of chlorotonil C2 but are consistent with chlorination plus an additional methylation event (Figure S12). MS fragmentation of the two compounds disclosed the methyl position to be C2 of chlorotonil C2 (data not shown). These results imply that cyclic chlorotonil precursor molecules are chlorinated prior to methylation at C2 and that precursor molecules that are already methylated at C2 are not accepted as substrates by CtoA. The existence of mono- and dichlorinated C2-methyl derivatives hints that the methylation and the chlorination process are carried out almost in parallel. Further support for this model came from the analysis of wild-type *So* ce1525 extracts for the corresponding chlorotonil derivatives: in addition to chlorotonil A (479.17 *m/z*, $[M + H]^+$) and chlorotonil B (445.21 *m/z*, $[M + H]^+$), the equivalent nonmethylated derivatives (465.15 *m/z*, $[M + H]^+$; 431.19 *m/z*, $[M + H]^+$) as well as the nonmethylated and nonchlorinated precursor (397.23 *m/z*, $[M + H]^+$) were detected (**8**, **9**, **10** in Figure S13).

To further exploit the functionality of CtoA, a feeding experiment with the natural producer strain *So* ce1525 was carried out. The chlorine source in the media was depleted and replaced with equimolar amounts of the respective bromide salt, which was achieved by exchanging the media component calcium chloride for calcium bromide. As anticipated, substantial amounts of new brominated compounds were biosynthesized (**11**, **12** in Figure S14). Consistent with a lack of chloride, only trace amounts of chlorotonil A and B were produced, while the nonmethylated, nonhalogenated precursor molecule **10** ($[M + H]^+ = 397.23$) accumulated. We thus conclude that CtoA is also capable of conducting bromination reactions.

Given the promising bioactivity seen for the dichloro-derivative of anthracimycin, a biological producer of this

compound would be of great interest. We thus elaborated a strategy for integration of *ctoA* under regulation of an *ermE* promoter into the *attB* site of the natural producer *Streptomyces* sp. CNH365, despite legitimate doubts as to the ability of CtoA to transform anthracimycin given its methylation pattern. Despite difficulty in finding conditions for genetic modification of *Streptomyces* sp. CNH365, two mutants harboring the *ctoA* gene were eventually obtained. After verification of the genotype by PCR, the mutants were grown in liquid media and extracts were prepared as described by Jang et al.³³ However, despite exhaustive LCMS analysis, no evidence for the production of halogenated anthracimycin analogues could be found. Given our findings regarding its substrate specificity, we conclude that anthracimycin, being methylated at C2, is not a substrate for CtoA.

Comparative Analysis of the *atc* Biosynthetic Gene Cluster and a Model for Anthracimycin Biosynthesis.

The structure of anthracimycin, a bioactive natural product isolated from a marine streptomycete,³³ closely resembles that of chlorotonil. We therefore set out to identify the anthracimycin biosynthetic gene cluster for comparison of the two pathways. Genome sequencing of the natural producer strain *Streptomyces* sp. CNH365 using the Illumina technique yielded 72 scaffolds which were subjected to automatic secondary metabolite pathway annotation using antiSMASH3.³⁴ In addition, the genome sequence was searched with BLAST using the chlorotonil PKS genes as the query sequence. Surprisingly, this search revealed the presence of two identical copies of a *trans*-AT PKS gene cluster in the genome of *Streptomyces* sp. CNH365 that were highly likely to encode the anthracimycin biosynthetic machinery (Figure S15). This peculiarity is rarely seen, and the circumstances of its origin are beyond the scope of this work. However, the presence of a duplicated biosynthetic gene cluster suggests that production of anthracimycin may provide a significant selection advantage. The genomic loci each span 70 kb and consist of three large PKS encoding genes (*atcD*, *atcE*, *atcF*), a tandem AT gene with a C-terminal ER domain (*atcC*), and several genes up- and downstream from the PKS core region encoding transport or regulator functions (Table 3). The core gene cluster could be determined as a 53 kb region spanning the genes *atcA*–*atcI* by comparison with the anthracimycin biosynthetic gene cluster of *Streptomyces* sp. T676, which is reported by Alt and Wilkinson contemporaneously with this article (this issue). At first glance, the organization of this gene cluster is similar to that of the chlorotonil biosynthetic gene cluster (Figure 3). The most obvious difference is the absence of genes encoding homologues for the halogenase CtoA and the free-standing methyltransferase CtoF which agrees well with the chemical structure of anthracimycin in comparison to chlorotonil. In addition to these major differences, the domain distribution among the *atcDEF* genes differs from the arrangement seen for *ctoCDE*; this is discussed in section S8.2 of the Supporting Information.

The architectural irregularities of the anthracimycin PKS (versus that anticipated from a retro-biosynthetic analysis) raise questions about how it produces a chemical scaffold so similar to chlorotonil. While the chlorotonil PKS also shows unusual domain arrangements, these peculiarities are not dissimilar to those often seen for *trans*-AT PKS systems. In contrast, the anthracimycin biosynthetic machinery appears to lack several domains while others are placed distantly from the anticipated point of action. We are nevertheless confident that the *atc* locus represents the anthracimycin biosynthesis gene cluster as

Table 3. Proposed Function of the Genes Involved in Anthracimycin Biosynthesis and the Surrounding Open Reading Frames

gene/protein	length (bp/aa)	proposed function			accession number (GenBank)
		proposed function of homologous protein	source of the homologous protein	identity/similarity, %	
<i>atcC</i> / <i>AtcC</i>	3222/1074	AT ₁ (45–796), AT ₂ (927–1767), ER (1944–2709)	<i>Streptomyces</i> sp. CNS654	82/88	WP_032767193
<i>atcD</i> / <i>AtcD</i>	3462/1154	KS ₁ (54–1329), KR ₁ (3625–4180), ACP ₁ (4459–4660), ACP ₃ (15153–13690), MT ₁ (14344–14989), ACP ₃ (15157–15349), ER ₃ (15568–16492), KS ₄ (16603–17875), DH ₄₋₁ (17974–18337), DH ₄₋₂ (18382–19206)	<i>Streptomyces ambiofaciens</i>	82/87	CAI78131
<i>atcE</i> / <i>AtcE</i>	18816/6272	ACP ₄ (147–355), KS ₅ (493–1777), DH ₅ (2317–3141), KR ₅ (3928–4480), ACP ₅ (4759–4960), KS ₆ (5128–6412), ACP ₆₋₁ (6601–6793), ACP ₆₋₂ (7375–7585), KS ₇ (7747–9022), DH ₇ (9532–10356), KR ₇ (10951–11488), MT ₇ (12142–12796), ACP ₇ (12883–13087)	<i>Streptomyces violaceusniger</i>	70/74	WP_014060436
<i>atcF</i> / <i>AtcF</i>	22806/7602	KS ₈ (145–1417), DH ₈ (1981–2805), KR ₈ (3487–4033), ACP ₈ (4273–4480), KS ₉ (4651–5944), ACP ₉ (6892–7066), KS ₁₀ (7237–8542), ACP ₁₀ (9178–9364), TE (9508–10312), MT ₁₀ (10783–11422)	<i>Streptomyces</i> sp. CNQ431	63/69	WP_033952594
			<i>Micromonospora lupini</i>	36/46	WP_007461885
			<i>Streptomyces</i> sp. CNR698	54/68	WP_027732177
			<i>Methanocella arvorizae</i>	55/73	WP_012036133
			<i>Peanibacillus</i> sp. OSY-SE	29/44	WP_036705498
			<i>Streptomyces</i> sp. NRRL F-5065	80/90	WP_037857030
			<i>Streptomyces pristinaespiralis</i>	77/78	WP_005322088
			<i>Streptomyces albus</i>	79/78	WP_030624822
Orf1	837/279	regulator			
Orf2	1533/511	putative amino acid transporter			
Orf3	516/172	hypothetical protein			
Orf4	702/234	transposase			
<i>atcA</i> / <i>AtcA</i>	1593/531	putative multidrug efflux protein			
<i>atcB</i> / <i>AtcB</i>	615/205	TetR family transcriptional regulator			
<i>atcG</i> / <i>AtcG</i>	852/284	ATP binding protein			
<i>atcH</i> / <i>AtcH</i>	750/250	ABC transporter permease			
<i>atcI</i> / <i>AtcI</i>	708/236	hypothetical protein (partial)			
Orf5	309/103	PadR family transcriptional regulator			
Orf6	1278/426	transporter			

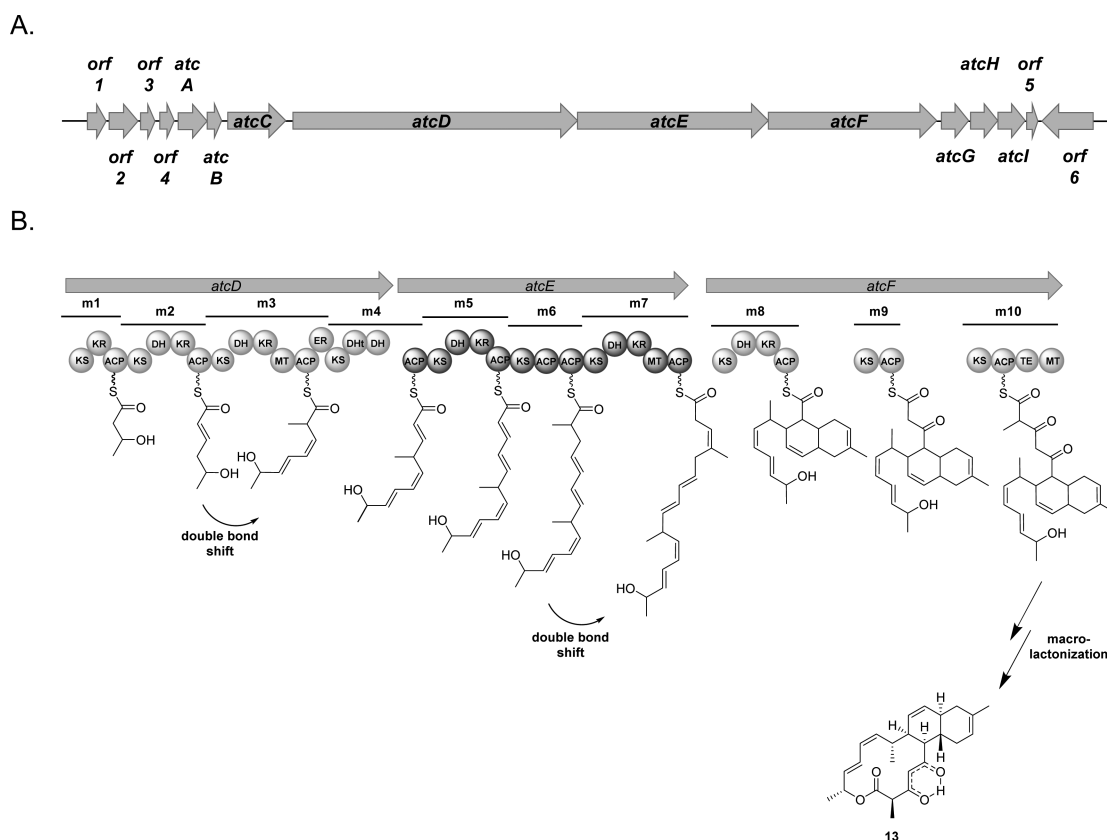


Figure 3. Model for anthracimycin biosynthesis in *Streptomyces* CNH365. A depicts the organization of the biosynthetic gene cluster. The proposed biosynthetic pathway for anthracimycin is shown in B. ACP, acyl carrier protein; DH, dehydratase, DHT, inactive truncated dehydratase; ER, enoyl reductase; KR, keto reductase; KS, keto synthase; MT, methyl transferase; TE, thioesterase.

careful inspection of the *Streptomyces* sp. CNH365 genome sequence did not afford any other candidate gene cluster encoding an alternative biosynthetic pathway for anthracimycin. A pathway for anthracimycin biosynthesis is proposed in section S8.3 of the Supporting Information.

Conclusion. In this study, we identified the biosynthetic gene clusters for chlorotonil and anthracimycin, two strikingly similar natural product scaffolds produced by a myxobacterium and a marine streptomycete, respectively. Our results indicate that both compounds are formed by *trans*-AT PKS pathways, and in-depth analysis of the *cto* and *atc* gene clusters allowed us to substantiate the reasons for several distinct structural features of chlorotonil A. In particular, the gene set for tailoring reactions readily explains the observed halogenation and methylation pattern of chlorotonil A, and a combination of gene inactivation and feeding experiments enabled us to propose a model for the order and timing of these post-PKS reactions. Both chlorotonil and anthracimycin apparently undergo [4 + 2] cycloadditions to form their characteristic decalin moiety, and we hypothesize that ring closure takes place during biosynthesis without catalysis by a dedicated “Diels–Alderase.” This notion is supported by the genome-wide absence of plausible candidates exhibiting similarity to any previously reported genes encoding such functionality. The finding that for anthracimycin in comparison to chlorotonil all stereocenters are inverted is very intriguing, and we hypothesize that the alternate steric arrangements induced by the C16-methyl group of the PKS intermediates acts to “pre-organize” the PKS-bound intermediates in advance of the [4 + 2] cyclization reactions (see Figure S11.2). The hydroxyl group introduced during the first round of chain extension is also of

opposite stereochemistry in each molecule, and this may also suggest a role in preorganizing the PKS bound intermediate. It is also conceivable that the orientation of the ACP-bound intermediates is predefined by the protein itself.

Despite them being far less conceptual than *cis*-AT PKS, several rules for polyketide assembly by *trans*-AT PKS were deduced from phenomena repetitively observed for these systems. However, urgent questions emerging from our comparative gene cluster analysis presented in this study could not be answered by what is known from *trans*-AT PKS studied to date. This suggests that generally valid rules for polyketide biosynthesis by these tessellated biosynthetic machineries are hard to establish.

Considering the promising bioactivity of chlorotonil A, the production of less lipophilic derivatives based on a system for heterologous expression of the pathway is one of the major goals to achieve in further studies. Analysis of the chlorotonil biosynthetic gene cluster provides valuable insights into chlorotonil biosynthesis, and the data gathered in this study is giving direction for the production of chlorotonil derivatives. Molecular features required for bioactivity of the compound as well as structural prerequisites for the production of chlorotonil derivatives were identified. Consequently, starting points for modification of the chlorotonil biosynthetic gene cluster toward production of new bioactive and less lipophilic derivatives could be concluded from this work.

EXPERIMENTAL SECTION

Bacterial Strains and Culture Conditions. *Sorangium cellulosum* So ce1525 was grown at 30 °C and 180 rpm in liquid H media (soy

flour 0.2%, glucose 0.2%, starch 0.8%, yeast extract 0.2%, $\text{CaCl}_2 \cdot 2\text{H}_2\text{O}$ 0.1%, $\text{MgSO}_4 \cdot 7\text{H}_2\text{O}$ 0.1%, HEPES 1.2%, pH 7.4) supplemented with 8 mg/L Fe-EDTA after autoclaving and on solid H agar plates (H media with 1.5% agar). In liquid culture, the strain was grown for 7 to 12 days. *Escherichia coli* strains were cultured in LB media (lysogeny broth; tryptone 1%, yeast extract 0.5%, sodium chloride 0.5%) at 37 °C until the required cell density was reached. If necessary, the appropriate antibiotics were added to the media for selection. *Streptomyces* CNH 365 was cultivated in liquid media as described previously.⁶ For maintenance, the strain was kept on SM agar plates (soy flour 2%, mannitol 2%) and incubated at 30 °C.

Preparation of Genomic DNA and PCR. So ce1525 genomic DNA was prepared either by phenol/chloroform/isoamylalcohol extraction³⁶ or with the help of the Gentra Puregene Genomic DNA Purification Kit (Qiagen) according to the manufacturer's protocol. Plasmid DNA was prepared by alkaline lysis or—if higher purity was required—using the GeneJET Plasmid Miniprep Kit (Thermo Scientific). PCR reactions were carried out in an Eppendorf mastercycler pro using the following program: 5 min initial denaturation (5 min at 98 °C) followed by 30 cycles of denaturation (98 °C, 20 s), annealing (58–68 °C, 30 s), and elongation (0.5–1.5 min according to the expected amplicon size). Final extension (5 min, 72 °C) ended the program. PCR amplicons were analyzed by gel electrophoresis and isolated by using the peqGOLD Gel Extraction Kit (Peqlab). PCR fragments were cloned into pJET 1.2 blunt (Thermo scientific) and sequenced by using the pJET1.2For/pJET1.2Rev sequencing primers.

Construction of a So ce1525 Cosmid Library. Genomic DNA of So ce1525 was partially digested using *Sau*3A1 as described in the Supercos1 manual (Agilent). A 2 μL fraction of each sample was analyzed by gel electrophoresis on an 0.35% agarose gel. Samples exhibiting the correct size distribution were combined, extracted, and dephosphorylated according to the Supercos1 manual. The Supercos1 vector was prepared as indicated in the respective manual. Complete digestion of the vector—indicated by the appearance of a 1.1 kb and a 6.5 kb band—was checked by agarose gel electrophoresis. For ligation of the partially digested DNA with the Supercos1 backbone, DNA and Supercos1 were used in a 2.5:1 ratio. The ligation preparation was shortly mixed, spun down, and incubated overnight at 4 °C. The ligation mix was afterward precipitated and packaged according to the manufacturer's instructions using the Gigapack III Gold (Agilent) packaging mixture. The resulting packaging mixture was used to infect *E. coli* HS996 cells that were subsequently plated out on LB agar plates supplemented with 50 $\mu\text{g}/\text{mL}$ ampicillin. Clones obtained after this selection were transferred into 384 well plates containing 2YT freezing media (tryptone 1.6%, yeast extract 1.0%, sodium chloride 0.5%, $\text{MgSO}_4 \cdot 7\text{H}_2\text{O}$ 0.068%, sodium citrate $\cdot 2\text{H}_2\text{O}$ 0.4%, $(\text{NH}_4)_2\text{SO}_4$ 0.81%, Glycerol 39.6%, K_2HPO_4 4.23%, KH_2PO_4 1.62%) and grown overnight at 30 °C. High-density colony filters of the 1865 Cosmid-containing library were generated by spotting cell suspension from every well onto LB soaked nitrocellulose membrane filters that were placed on LB ampicillin agar plates and incubated overnight at 30 °C. For spotting, a Qpix robot (Genetix, New Milton, Hampshire, UK) was used. The clones grown on the filter membrane were lysed (lysis solution: 0.5 M NaOH, 1.5 M NaCl). Cell debris was washed off, and the membranes were dried. The dried membranes were then immersed in 2 \times SSC (NaCl 0.3 M, tri-Sodiumcitrat $\cdot 2\text{H}_2\text{O}$ 0.03 M) for 5 min, drained, then covered with proteinase K solution and wrapped in aluminum foil. After 2 h of incubation at 37 °C, the membranes were carefully rinsed with water and air-dried on whatcan paper. The DNA was thus fixated on the membranes, which subsequently underwent a screening procedure.

Screening of the *Sorangium cellulosum* So ce1525 Cosmid Library for the Chlorotoniol Biosynthetic Gene Cluster. The cosmid library was screened using three probes targeting the 5'-end (halo probe), the 3'-end (TE probe), and the core region of the gene cluster. The probes were amplified from genomic DNA of So ce1525. For the halo probe, the primers halo_fwd (5'-CTCCTCCAGGTACCTCCG-CATCTC-3') and halo_rev (5'-CCGAGGAGCTCATGCAGCAGAC-3')

were used, for the core probe core_fwd (5'-GCAGGCGGTGTCCCTGC-ACGAC-3') and core_rev (5'-CATCCCGCTCAACAACCGAGGCAG-3') were used, and for the TE probe, TE_fwd (5'-CTCATCAT-GAGTCCAGGTACGCTC-3') and TE_rev (5'-CGGCGGGA-GATCTGCGCTGTCG-3') were used. Positive cosmids identified in this way were further analyzed by end-sequencing with the T3 and T7 primers. After this, the three most promising candidates (cosmid B8, D20, J23) were completely sequenced with the Illumina method. The thus obtained sequencing data were assembled and resulted in a 80 kb genomic region covering the sought biosynthetic gene cluster as well as additional sequence information upstream and downstream from this genomic region.

Construction of Myxobacterial Mutants by Insertional Mutagenesis. For targeted inactivation of genes within the chlorotoniol biosynthetic gene cluster, a 1 kb homologous region of the respective gene was amplified from So ce1525 genomic DNA by PCR using the required primers. The thus amplified DNA fragment was ligated to pSUPHyg and subsequently transformed into *E. coli* ET12567 harboring the pUB307 helper plasmid. The construct was then transferred into *Soc*e1525 by conjugation as described previously.³⁷ Obtained mutants were genotypically verified by PCR. Additionally phenotypic analysis was carried out as described below.

Construction of *Streptomyces* Mutants by Insertional Mutagenesis. For insertion of the chlorotoniol halogenase into the attB site of the *Streptomyces* genome, the halogenase gene was amplified from the So ce1525 genome using the pErmE-Hal_CNH365_fwd (5'-CAGATGATATCGATGCTGTTGTGGGCACAA-TCGTGCCGGTTGGTAGGATCCAGCGGCGGTCA-GAGAAGGGAGCGGAAATGGAAGCGAACCCCTGCA-3') and Hal_CNH365_rev (5'-ACATCTAGATCAGGCCGACACCTCCCGAAG-3') primers. An ermE promoter sequence was attached to the fwd primer. The thus amplified DNA fragment was cloned into pSET152; the resulting construct was transformed into *E. coli* ET12567 harboring the pUZ8002 helper plasmid. The construct was transferred into *Streptomyces* by conjugation as described by Hopwood et al.³⁸ Obtained mutants were genotypically verified by PCR. Additionally phenotypic analysis was carried out as described below.

Phenotypic Analysis of Myxobacterial Wildtype and Mutant Strains. For phenotypic analysis, the respective So ce1525 strains were grown in a 50 mL liquid culture on an orbital shaker (30 °C, 180 rpm) in autolaved H media. After 3 days of cultivation, 2% autoclaved absorber resin XAD16 was added to the cultures. Cells and XAD were harvested after 10 days of cultivation by centrifugation (10 min, 8000 rpm); the obtained pellet consisting of cells and XAD was frozen at -20 °C and subsequently freeze-dried. Pellets were extracted with 30 mL of methanol and three portions of acetone (30 mL). The acetone fractions were combined and evaporated. The remaining residue was dissolved in chloroform. For HPLC-MS measurements, the chloroform sample was diluted 1:100 in methanol.

Phenotypic Analysis of *Streptomyces* Wildtype and Mutant Strains. For phenotypic analysis of *Streptomyces* CNH365, the strains were grown in a 50 mL liquid culture in autoclaved CNH365 media. After 7 days of incubation at 28 °C and 200 rpm, 2% XAD16 was added, and the culture was shaken at 200 rpm and 28 °C for another 2 h. After 7 days of cultivation, mycelium and XAD were spun down at RT (10 min, 8000 rpm). The supernatant was discarded, and the pellet was washed with desalted water. The mycelium was resuspended and separated from the XAD by filtration through a XAD sieve. To extract anthracimycin and its derivatives, the XAD was extracted with three portions of acetone (30 mL each) for 20 min, respectively. The combined acetone fractions were evaporated, and the resulting residue was dissolved in 1 mL of chloroform. For HPLC-MS measurements, the chloroform sample was diluted 1:100 in methanol.

■ FEEDING STUDIES

For feeding of [¹³C-methyl] methionine, a sterile aqueous [¹³C-Methyl] methionine stock was produced (1 mg mL⁻¹). Three equal cultures were fed with six portions of the stock solution starting with 200 μL on the second day, 100 μL on the fourth day, and another 50 μL every second day. The cultures were grown for 10 days, while after 5 days

2% XAD16 was added. All feeding studies were carried out in triplicate.

The mutant strain So ce1525 *CtoAT::pKJAT12*, which does not produce Chlorotoniol A or any of its derivatives anymore, was grown in 20 mL of H-media supplemented with hygromycin at 100 $\mu\text{g/mL}$. A total of 1 mg of chlorotoniol C2 was suspended in 500 μL of DMSO and added to the liquid culture in four portions. On the third day, 250 μL of stock solution was added to the culture. On day five, 125 μL stock solution was added to the cultures, and on the following 2 days, 62.5 μL was fed to the culture. After another 24 h of incubation, 2% XAD absorber resin was added to the culture. Cells and XAD were harvested by centrifugation on day 10. Freeze-dried cell pellets were extracted with methanol and acetone and subjected to HPLC MS measurements. A nonfed control sample was run in parallel. The feeding study with chlorotoniol B was carried out the same way.

Bioactivity Testing of Chlorotoniol a and Its Congeners. All microorganisms were handled according to standard procedures and were obtained from the German Collection of Microorganisms and Cell Cultures (*Deutsche Sammlung für Mikroorganismen und Zellkulturen*, DSMZ) or were part of our internal strain collection. For microdilution assays, overnight cultures of *E. coli*, *M. luteus*, *B. subtilis*, and *S. aureus* in Müller-Hinton broth (0.2% beef infusion, 0.15% corn starch, 1.75% casein peptone; pH 7.4) and *E. faecalis* and *S. pneumoniae* in Tryptic soy broth (1.7% tryptone, 0.3% soytone, 0.5% NaCl, 0.25% K_2HPO_4 , 0.25% glucose; pH 7.3; microaerophilic growth conditions) were diluted in the growth medium to achieve a final inoculum of ca. 10^6 cfu/mL. Serial dilutions of chlorotonils in THF/Cremophor EL 1:1 were prepared from CHCl_3 stocks (10 mg mL^{-1}) in sterile 96-well plates. The cell suspension was added, and microorganisms were grown for 16–24 h at 37 °C. Growth inhibition was assessed in two independent experiments by visual inspection, and given MIC (minimum inhibitory concentration) values are the lowest concentration of antibiotic at which no visible growth was observed.

The MTT assay for determination of the cytotoxicity of chlorotoniol A against human cell lines was carried out as described by Herrmann et al.³⁹

■ ASSOCIATED CONTENT

■ Supporting Information

The Supporting Information is available free of charge on the ACS Publications website at DOI: 10.1021/acscchembio.5b00523.

Additional details for analytical and experimental procedures (PDF)

Accession Codes

atc_biosynthetic_gene_cluster, KT368179; cto_biosynthetic_gene_cluster, KT368180

■ AUTHOR INFORMATION

Corresponding Author

*E-mail: rom@mx.uni-saarland.de.

Notes

The authors declare no competing financial interest.

■ ACKNOWLEDGMENTS

The authors would like to thank W. Kessler and S. Bernecker and their team for large-scale fermentation, K. Schober for skillful assistance in the isolation of the structural variants of chlorotoniol A and C. Kakoschke for NMR measurements. We are grateful to M. Hoffmann and. Hoffmann for HPLC-MS measurements and V. Schmitt and J. Herrmann for bioactivity assays.

■ REFERENCES

- (1) Koehn, F. E., and Carter, G. T. (2005) The evolving role of natural products in drug discovery. *Nat. Rev. Drug Discovery* 4, 206–220.
- (2) Wenzel, S. C., and Müller, R. (2005) Recent developments towards the heterologous expression of complex bacterial natural product biosynthetic pathways. *Curr. Opin. Biotechnol.* 16, 594–606.
- (3) Gerth, K., Pradella, S., Perlova, O., Beyer, S., and Müller, R. (2003) Myxobacteria: Proficient producers of novel natural products with various biological activities - Past and future biotechnological aspects with the focus on the genus *Sorangium*. *J. Biotechnol.* 106, 233–253.
- (4) Schneiker, S., Perlova, O., Kaiser, O., Gerth, K., Alici, A., Altmeyer, M. O., Bartels, D., Bekel, T., Beyer, S., Bode, E., Bode, H. B., Bolten, C. J., Choudhuri, J. V., Doss, S., Elnakady, Y. a, Frank, B., Gaigalat, L., Goesmann, A., Groeger, C., Gross, F., Jelsbak, L., Jelsbak, L., Kalinowski, J., Kegler, C., Knauber, T., Konietzny, S., Kopp, M., Krause, L., Krug, D., Linke, B., Mahmud, T., Martinez-Arias, R., McHardy, A. C., Merai, M., Meyer, F., Mormann, S., Muñoz-Dorado, J., Perez, J., Pradella, S., Rachid, S., Raddatz, G., Rosenau, F., Rückert, C., Sasse, F., Scharfe, M., Schuster, S. C., Suen, G., Treuner-Lange, A., Velicer, G. J., Vorhölter, F.-J., Weissman, K. J., Welch, R. D., Wenzel, S. C., Whitworth, D. E., Wilhelm, S., Wittmann, C., Blöcker, H., Pühler, A., and Müller, R. (2007) Complete genome sequence of the myxobacterium *Sorangium cellulosum*. *Nat. Biotechnol.* 25, 1281–1289.
- (5) Gerth, K., Steinmetz, H., Höfle, G., and Jansen, R. (2008) Chlorotoniol A, a Macrolide with a Unique gem-Dichloro-1, 3-dione Functionality from *Sorangium cellulosum*, So ce1525. *Angew. Chem., Int. Ed.* 47, 600–602.
- (6) Jang, K. H., Nam, S.-J., Locke, J. B., Kauffman, C. a, Beatty, D. S., Paul, L. a, and Fenical, W. (2013) Anthracimycin, a potent anthrax antibiotic from a marine-derived actinomycete. *Angew. Chem., Int. Ed.* 52, 7822–4.
- (7) Piel, J. (2010) Biosynthesis of polyketides by trans-AT polyketide synthases. *Nat. Prod. Rep.* 27, 996–1047.
- (8) Held, J., Gebru, T., Kalesse, M., Jansen, R., Gerth, K., Müller, R., and Mordmüller, B. (2014) Antimalarial activity of the myxobacterial macrolide chlorotoniol a. *Antimicrob. Agents Chemother.* 58, 6378–84.
- (9) Musiol, E. M., Greule, A., Härtner, T., Kulik, A., Wohlleben, W., and Weber, T. (2013) The AT₂ domain of KirCI loads malonyl extender units to the ACPs of the kirromycin PKS. *ChemBioChem* 14, 1343–52.
- (10) Musiol, E. E. M., and Weber, T. (2012) Discrete acyltransferases involved in polyketide biosynthesis. *MedChemComm* 3, 871.
- (11) Piel, J. (2002) A polyketide synthase-peptide synthetase gene cluster from an uncultured bacterial symbiont of *Paederus* beetles. *Proc. Natl. Acad. Sci. U. S. A.* 99, 14002–7.
- (12) Gurney, R., and Thomas, C. M. (2011) Mupirocin: Biosynthesis, special features and applications of an antibiotic from a Gram-negative bacterium. *Appl. Microbiol. Biotechnol.* 90, 11–21.
- (13) Perlova, O., Gerth, K., Kaiser, O., Hans, A., and Müller, R. (2006) Identification and analysis of the chivosazol biosynthetic gene cluster from the myxobacterial model strain *Sorangium cellulosum* So ce56. *J. Biotechnol.* 121, 174–191.
- (14) Weber, T., Laiple, K. J., Pross, E. K., Textor, A., Grond, S., Welzel, K., Pelzer, S., Vente, A., and Wohlleben, W. (2008) Molecular Analysis of the Kirromycin Biosynthetic Gene Cluster Revealed β -Alanine as Precursor of the Pyridone Moiety. *Chem. Biol.* 15, 175–188.
- (15) Bumpus, S. B., Magarvey, N. a, Kelleher, N. L., Walsh, C. T., and Calderone, C. T. (2009) *J. Am. Chem. Soc.* 130, 11614–11616.
- (16) Witkowski, A., Joshi, A. K., Lindqvist, Y., and Smith, S. (1999) Conversion of a ??-ketoacyl synthase to a malonyl decarboxylase by replacement of the active-site cysteine with glutamine. *Biochemistry* 38, 11643–11650.
- (17) Nguyen, T., Ishida, K., Jenke-Kodama, H., Dittmann, E., Gurgui, C., Hochmuth, T., Taudien, S., Platzer, M., Hertweck, C., and Piel, J. (2008) Exploiting the mosaic structure of trans-acyltransferase

polyketide synthases for natural product discovery and pathway dissection. *Nat. Biotechnol.* 26, 225–33.

(18) Keatinge-Clay, A. T. (2007) A tylosin ketoreductase reveals how chirality is determined in polyketides. *Chem. Biol.* 14, 898–908.

(19) Caffrey, P. (2003) Conserved amino acid residues correlating with ketoreductase stereospecificity in modular polyketide synthases. *ChemBioChem* 4, 654–657.

(20) Keatinge-Clay, A. (2008) Crystal structure of the erythromycin polyketide synthase dehydratase. *J. Mol. Biol.* 384, 941–53.

(21) Pistorius, D., and Müller, R. (2012) Discovery of the rhizopodin biosynthetic gene cluster in *Stigmatella aurantiaca* Sg a15 by genome mining. *ChemBioChem* 13, 416–26.

(22) Kusebauch, B., Busch, B., Scherlach, K., Roth, M., and Hertweck, C. (2010) Functionally distinct modules operate two consecutive $\alpha,\beta \rightarrow \beta,\gamma$ double-bond shifts in the rhizoxin polyketide assembly line. *Angew. Chem.* 122, 1502–1506.

(23) Moldenhauer, J., Götz, D. C. G., Albert, C. R., Bischof, S. K., Schneider, K., Süßmuth, R. D., Engeser, M., Gross, H., Bringmann, G., and Piel, J. (2010) The Final Steps of Bacillaene Biosynthesis in *Bacillus amyloliquefaciens* FZB42: Direct Evidence for β,γ Dehydration by a trans-Acyltransferase Polyketide Synthase. *Angew. Chem.* 122, 1507–1509.

(24) Calderone, C. T. (2008) Isoprenoid-like alkylations in polyketide biosynthesis. *Nat. Prod. Rep.* 25, 845–53.

(25) Gu, L., Eisman, E. B., Dutta, S., Franzmann, T. M., Walter, S., Gerwick, W. H., Skiniotis, G., and Sherman, D. H. (2011) Tandem acyl carrier proteins in the curacin biosynthetic pathway promote consecutive multienzyme reactions with a synergistic effect. *Angew. Chem., Int. Ed.* 50, 2795–8.

(26) Crosby, J., and Crump, M. P. (2012) The structural role of the carrier protein–active controller or passive carrier. *Nat. Prod. Rep.* 29, 1111–37.

(27) Gay, D. C., Gay, G., Axelrod, A. J., Jenner, M., Kohlhaas, C., Kampa, A., Oldham, N. J., Piel, J., and Keatinge-Clay, A. T. (2014) A close look at a ketosynthase from a trans-acyltransferase modular polyketide synthase. *Structure* 22, 444–451.

(28) Auclair, K., Sutherland, A., Kennedy, J., Witter, D. J., Van Den Heever, J. P., Hutchinson, C. R., Vederas, J. C., Tg, C., Uni, V., August, R. V., and Although, A. (2000) Lovastatin Nonaketide Synthase Catalyzes an Intramolecular Diels–Alder Reaction of a Substrate Analogue. *J. Am. Chem. Soc.* 122, 11519–11520.

(29) Kim, H. J., Ruszczycky, M. W., Choi, S., Liu, Y., and Liu, H. (2011) Enzyme-catalysed [4 + 2] cycloaddition is a key step in the biosynthesis of spinosyn A. *Nature* 473, 109–12.

(30) Serafimov, M., Gillingham, D., Kuster, S., and Hilvert, D. (2008) *J. Am. Chem. Soc.* 130, 7798–7799.

(31) Katayama, K., Kobayashi, T., Chijimatsu, M., Ichihara, A., and Oikawa, H. (2008) Purification and N-terminal amino acid sequence of solanapyrone synthase, a natural Diels–Alderase from *Alternaria solani*. *Biosci., Biotechnol., Biochem.* 72, 604–7.

(32) Hashimoto, T., Hashimoto, J., Teruya, K., Hirano, T., Shin-Ya, K., Ikeda, H., Liu, H.-W., Nishiyama, M., and Kuzuyama, T. (2015) Biosynthesis of Versipelostatin: Identification of an Enzyme-Catalyzed [4 + 2]-Cycloaddition Required for Macrocyclization of Spirotetronate-Containing Polyketides. *J. Am. Chem. Soc.* 137, 572–575.

(33) Jang, K. H., Nam, S.-J., Locke, J. B., Kauffman, C. a., Beatty, D. S., Paul, L. a., and Fenical, W. (2013) Anthracimycin, a Potent Anthrax Antibiotic from a Marine-Derived Actinomycete. *Angew. Chem.* 125, 7976–7978.

(34) Weber, T., Blin, K., Duddela, S., Krug, D., Kim, H. U., Brucoleri, R., Lee, S. Y., Fischbach, M. a., Muller, R., Wohlleben, W., Breitling, R., Takano, E., and Medema, M. H. (2015) antiSMASH 3.0—a comprehensive resource for the genome mining of biosynthetic gene clusters. *Nucleic Acids Res.* 43, W237–W243.

(35) Irschik, H., Kopp, M., Weissman, K. J., Buntin, K., Piel, J., and Müller, R. (2010) Analysis of the sorangicin gene cluster reinforces the utility of a combined phylogenetic/retrobiosynthetic analysis for deciphering natural product assembly by trans-AT PKS. *ChemBioChem* 11, 1840–9.

(36) Green, M. R., and Sambrook, J. *Molecular Cloning: A Laboratory Manual*. Cold Spring Harbor Laboratory Press, Cold Spring Harbor, NY.

(37) Kopp, M., Irschik, H., Gross, F., Perlova, O., Sandmann, A., Gerth, K., and Müller, R. (2004) Critical variations of conjugational DNA transfer into secondary metabolite multiproducing *Sorangium cellulosum* strains So ce12 and So ce56: Development of a mariner-based transposon mutagenesis system. *J. Biotechnol.* 107, 29–40.

(38) Kieser, T., Bibb, M. J., Buttner, M. J., and Chater, K. F. (2000) *Practical Streptomyces Genetics*, John Innes Foundation, Norwich, England.

(39) Herrmann, J., Elnakady, Y. a., Wiedmann, R. M., Ullrich, A., Rohde, M., Kazmaier, U., Vollmar, A. M., and Müller, R. (2012) Pretubulysin: From hypothetical biosynthetic intermediate to potential lead in tumor therapy. *PLoS One* 7, 1–12.